

Original Article

IN SILICO ANALYSIS OF STRUCTURAL REQUIREMENTS FOR THIOPHENE DERIVATIVES AGAINST POLO LIKE KINASE-1 (PLK1)

SHRAVAN KUMAR GUNDA*, VIJAYA LAKSHMI LOKIREVU, SHYAMASUNDARA CHARY RUDROJU, SWATHI MUTYA, MAHMOOD SHAIK

Bioinformatics Division, Osmania University, Hyderabad 500007, Telangana State, India
Email: gunda14@gmail.com

Received: 02 Dec 2014 Revised and Accepted: 01 Jan 2015

ABSTRACT

Objective: Development of anti-mitotic drugs for chemotherapy of cancer has been one of the main focuses of research in 21st century. Present work aims to study the structural requirements of thiophene derivatives against PLK1 as a target for designing novel strategies for cancer chemoprevention. To understand the structural requirements that will lead to enhanced inhibitory potencies, we have carried out 3D-QSAR (quantitative structure-activity relationship) studies on a series of thiophene derivatives as PLK1 receptor inhibitors.

Methods: CoMFA, CoMSIA and molecular docking studies were performed on a series of thiophene derivatives as PLK1 receptor inhibitors using Sybyl 6.7.

Results: We have successfully derived statistically significant model from 100 thiophene derivatives and validated, it against an external test set of 34 compounds and 66 molecules used in the training set. The Co MFA model yielded q^2 -0.845, r^2 -0.978. While the Co MSIA model yielded q^2 -0.804, r^2 -0.968. The predictive ability of these models supported by docking studies; produced better docking scores and binding affinity to the specified target polo like kinase1 (3THB) and moreover, the 3D QSAR model used for suggesting the next-generation lead analogues.

Conclusion: 3D-QSAR has been established for a series of Polo like Kinase1 (PLK1) inhibitors employing the most widely used techniques CoMFA and CoMSIA. The conclusions derived from both models are similar and reliable. Docking studies are also performed to obtain the bioactive confirmations for the whole data-set. The obtained 3D contour maps along with the docking results provided a rational clue for the design of more favorable anti-mitotic agents. Overall, the structural modifications of the lead molecule have achieved to improve selective PLK1 inhibitory activity.

Keywords: Anti-mitotics, Thiophene derivatives against PLK1, 3D-QSAR, CoMFA, CoMSIA, Molecular Docking.

INTRODUCTION

Deregulation of cell cycle mechanism is a hallmark of cancer cell development. Mitosis regulatory genes or gene products play a pivotal role in the process of cell cycle prognosis [1]. Such features suggest that the cell cycle control or regulation play an important role in chemotherapy for cancer treatment [2]. Clinical use of anti-mitotics has been established as an effective approach to cancer therapy [3]. Polo like kinases are most commonly used targets for antimitotics, which are a group of serine\threonine kinase family that contains an amino-terminal serine / threonine kinase domain and carboxy-terminal polo box domain (s).

Although PLK family contains PLK₁, PLK₂ (SNK), PLK₃ (PRK/FNK), and PLK₄ (SAK), PLK₁ is well studied. It plays an important role during multiple stages of cell cycle and also involves in the regulation of mitotic progression, including mitotic regulatory entry, mitotic spindle formation, chromosome segregation, and cytokinesis [4, 5]. Improper regulation of PLK₁ activity gives rise to genetic instability, leading to oncogenic transformation [6].

Preclinical validation of PLK₁ as a cancer target has been demonstrated through the use of small interfering RNA in cell culture [7] and antisense oligonucleotides in mouse tumor xenograft models [8]. Finally, correlations between elevated PLK1 expression and poor prognosis in the clinical outcomes have been established [9]. Furthermore, Polo like kinases are involved in many malignancies/neoplastic diseases such as lung carcinomas [10], breast carcinomas [11], oropharyngeal carcinomas[12], papillary carcinomas [13], esophageal carcinomas [14], pancreatic carcinomas [15], ovarian carcinomas [16], colorectal carcinomas [17], prostate carcinomas [18] and melanomas [19]. Finally, emerging evidence of peak expression of PLK₁ in a variety of cancers suggesting towards, the discovery of more potent novel small-molecule inhibitors of PLK₁ against cancer.

Study design

Biological data

A series of thiophene derivative compounds having a promising effect to inhibit PLK₁ and selected as an anti-mitotic agent for 3D-QSAR and docking studies. The data-set of 100 PLK₁ inhibitors and the biological activities against PLK₁ has been taken from the literature [20-22]. All the sample's structures and *in vitro* inhibitory concentrations (IC₅₀) has mentioned in following table: 1 (a, b, c, d and e).

The total data-set of 100 compounds have divided into training-set for generating 3D-QSAR models and a test-set for validating the quality of the models. *In vitro* inhibitory concentrations (IC₅₀) of the molecules has converted into corresponding log of values (pIC₅₀) (pIC₅₀ = -logIC₅₀) and used as dependent variables in the present study of CoMFA and CoMSIA. A training-set of 66 molecules and a test-set of 34 molecules selection were done randomly in 3D-QSAR studies.

Structure building and minimization

Molecular modeling package of silicon graphics interface (SYBYL 6.7) was used to construct a data-set of 100 thiophene derivatives that has been collected from literature [20-22]. Energy minimization has performed to all the molecules using Tripos Force Field, and the charges are Gasteiger-Huckel with gradient convergence 0.005 kcal/mol. The semi-empirical AM1 Hamiltonian method of MOPAC package used for Geometry optimization.

Alignment procedure

Molecular alignment plays a vital role in 3D-qsar analysis. The accuracy of CoMFA and CoMSIA model prediction and contour analysis depends on the structural alignment of all the analogues. The molecular alignment has carried out by SYBYL align database option using the atom-based RMS fit method.

The most active compound (compound no: 14 according to the literature) used as template and the remaining 99 samples aligned to it

through using the basic core structure(5-(1H-benzimidazole-1-yl) thiophene-3-ol) and the alignment of all the molecules shown in fig. 1.

Table 1: Structure and biological activities as ionization concentration (IC₅₀)

Table 1(a): (1-12)

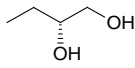
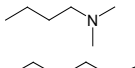
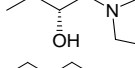
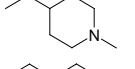
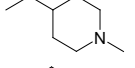
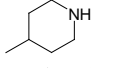
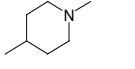
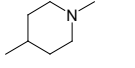
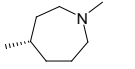
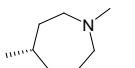
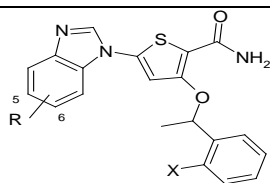
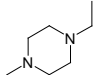
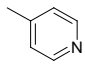
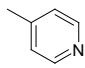
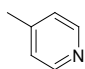
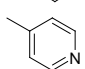
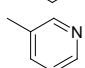
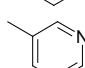
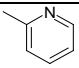
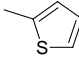
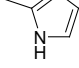
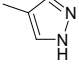
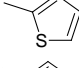
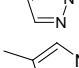
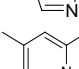
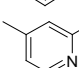
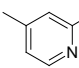
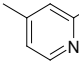
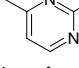
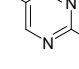
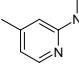
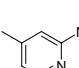
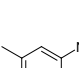
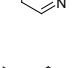
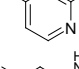
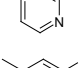
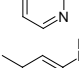
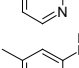
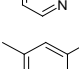
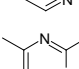
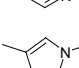
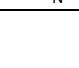
Compound number	X	R
1	Cl	Me
2	CF ₃	Me
3	Cl	
4	Cl	
5	Cl	
6	CF ₃	
7	Cl	
8	CF ₃	
9	CF ₃	
10	Cl	
11	Cl	
12	Cl	

Table 1(b): (13-49)



Compound number	X	Position	R
13	CF ₃	6	
14	Cl	5,6	Di-OMe
15	CF ₃	5	Ph
16	CF ₃	6	Ph
17	CF ₃	5	
18	CF ₃	6	
19	Cl	5	
20	Cl	6	
21	CF ₃	5	
22	CF ₃	6	

23	CF ₃	5	
24	CF ₃	5	
25	CF ₃	5	
26	CF ₃	5	
27	CF ₃	5	
28	Cl	5	
29	Cl	6	
30	CF ₃	5	
31	CF ₃	5	
32	CF ₃	6	
33	CF ₃	5	
34	CF ₃	5	
35	CF ₃	5	
36	Cl	5	
37	Cl	5	
38	CF ₃	5	
39	CF ₃	5	
40	CF ₃	5	
41	Cl	5	
42	Cl	5	
43	Cl	5	
44	Cl	5	
45	Cl	5	
46	Cl	5	

47	Cl	5	
48	Cl	5	
49	Cl	5	

Table 1(c): (80-84)

Compound number	R ₁	R ₂
50	H	-
51	2-Me	-
52	3-Me	-
53	4-Me	-
54	2-OMe	-
55	3-OMe	-
56	4-OMe	-
57	2-Cl	-
58	3-Cl	-
59	4-Cl	-
60	2-CF ₃	-
61	2-F	-
62	2-Br	-
63	2-Me	5-Cl
64	2-Me	6-Cl
65	2-Br	5-CF ₃
66	2-Br	6-CF ₃
67	2-CF ₃	5-SO ₂ Me
68	2-CF ₃	6-SO ₂ Me
69	2-CF ₃	5-OMe
70	2-CF ₃	6-OMe
71	2-CF ₃	5,6-Di-OMe
72	H	5,6-Di-OMe
73	2-Br	5,6-Di-OMe
74	2-Cl	5,6-Di-OMe
75	2-CN	5,6-Di-OMe
76	2-SO ₂ Me	5,6-Di-OMe
77	2-COMe	5,6-Di-OMe
78	2-O CF ₃	5,6-Di-OMe
79	2-OMe	5,6-Di-OMe
80	3-NMe ₂	5,6-Di-OMe
81	3-NH ₂	5,6-Di-OMe
82	4-OMe	5,6-Di-OMe
83	3-CN	5,6-Di-OMe
84	4-SO ₂ Me	5,6-Di-OMe

Table 1(d): (85-95)

Compound number	R
85	CH ₂ CH ₂ Ph
86	CH ₂ CH ₂ CH ₂ Ph
87	Cyclopentylmethyl
88	Cyclohexylmethyl
89	2-Thienylmethyl
90	3-Thienylmethyl
91	(3-Chloro)-2-Thienyl)methyl
92	2-Furylmethyl
93	3-Furylmethyl
94	4-Pyridinylmethyl
95	(2-Bromo-4-pyridinyl)methyl

3D-QSAR studies

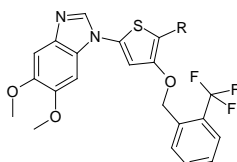
CoMFA

One of the most commonly used statistical approaches for quantitative structure activity relationship (QSAR) is the

comparative molecular field analysis (CoMFA). A good alignment is the single most important part to do CoMFA analysis. In CoMFA, each molecule is located within the automatically determined grid-space of 2.0 Å in x, y and Z planes through a grid box dimension. Steric and electrostatic indices calculated by using sp³ hybridized carbon atom having positive charge+1 (probe) with a distance

dependent dielectric constant 1.0, and the probe calculates the Leonard-Jones potential for steric fields and columbic potentials for electrostatic energy fields between the probe molecule and the other aligned molecules. These are calculated through the use of tripos force field. Energy truncation cut off used for both steric and electrostatic interactions is 30 kcal/mol. To improve the signal-to-noise ratio column filtering is adjusted as 2.0 kcal/mol by which we can omit those lattice points whose energy variation was below this threshold. Cross-validation and non-cross validation analysis was used for regression analysis with the optimum number of components. Standard error of estimate (SEE) and the F value also calculated. Interaction energies were measured and analyzed for a set of 3D structures and are used to establish QSAR.

Table 1(e): (96-100)



Compound number	R
96	CO ₂ H
97	CN
98	1H-Tetrazol-5-yl
99	CSNH ₂
100	COMe

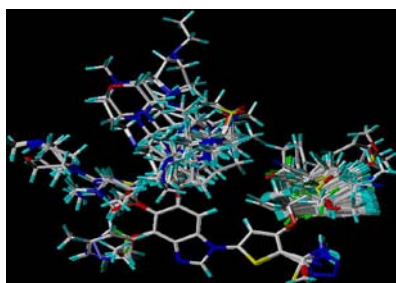


Fig. 1: Alignment of thiophene derivatives

CoMSIA

CoMSIA (comparative molecular similarity indices analysis) is developed based on similarity indices of five different descriptors of the molecules; steric, electrostatic, hydrophobic, hydrogen bond donor and hydrogen bond acceptor. CoMSIA computes the six descriptors by using the same lattice box defined in CoMFA. All five descriptors have evaluated at each lattice interaction of a regularly spaced grid of 2.0 Å. A probe (sp³ hybridized carbon) atom within the radius of 1 Å, +1 charge, hydrophobicity+1.0, and hydrogen bond donor and acceptor properties of +1.0 was used to evaluate steric, electrostatic, hydrogen bond donor, hydrogen bond acceptor and hydrophobic potential fields.

The predictive abilities of the developed models have determined by random division of all the 100 samples as training set and test set, and the biological activities are considered as a dependent column.

Partial least square (PLS) analysis

PLS is used to find the fundamental relations between the both X and Y matrices, i.e. a latent variable approach to modeling the covariance structures in these two spaces. The PLS algorithm was used to quantify the relationship between the structural parameters and the biological activities. Statistical analysis has implemented by applying the partial least square (PLS) procedure to the appropriate columns of the CoMFA and CoMSIA tables and utilizing the standard scaling method (CoMFA_STD). The PLS regression algorithm used the CoMFA/CoMSIA interaction energy fields as independent variables and the pIC₅₀ values as dependent variables. Standard

options are applied to calculate the regression analysis. Partial least squares have done by choosing Leave-one-out method and the column filtering as 2.0 kcal/mol.

Molecular docking

Ligand-based docking

To determine the probable similarities between the QSAR and the binding confirmations, and also to know the crucial interactions with the active site, docking has performed for all the aligned PLK₁ inhibitors. The SYBYL Flex X interface tool has utilized to perform molecular docking. The fast-automated docking program Flex X considers the conformational flexibility of lead molecules using an incremental construction algorithm. The incremental fragment placing technique is based on a greedy strategy combined with efficient methods for overlap detection and for the search of new interactions. In this method, the flexibility of the ligands has considered by including several conformations of ligands while maintaining a rigid structure for the receptor. By default, 30 conformations have generated for each molecule. The default parameters are selected. The resulting docked conformations are scored based on the strength of receptor-ligand interactions.

The 3Dimensional (crystal) structure of PLK₁ was obtained from the Protein Data Bank, having a PDB entry of 3THB. Hydrogen atoms (505) are added to the 3THB. Pockets identified by using Biopolymer, and the white pocket (having 9 possible interactive residues) has selected to predict the interactions of all the 100 lead molecules (for both training and test-set). The active site was defined within the radius of 6.5 Å. All the molecules docked score has given in the respective table: 2(a&b).

Molecular Docking also well supported the 3D-QSAR analysis with better docking scores having good interactions with the predefined active site.

RESULTS AND DISCUSSION

CoMFA and CoMSIA

The CoMFA and the CoMSIA methods are employed to create 3D-QSAR models for the training-set of 66 thiophene derivatives. The statistical results of the CoMFA and CoMSIA analyses are summarized in table: 2(c). The PLS analysis predictions of the CoMFA model are obtained as q₂ =0.978, r₂=0.845 while for CoMSIA q₂ =0.968, r₂=0.804 and the number of compounds used for both is 6. The results produced by CoMFA and CoMSIA are mostly same, indicating stable analyses of high quality. These results suggest that the present model is reliable and accurate. Actual and predicted activities achieved from CoMFA and CoMSIA models with the residuals, for all the aligned 100 molecules are shown in table: 2(a&b). The graph of real versus predicted pIC₅₀ values of the training and the test-set molecules for CoMFA and CoMSIA models are depicted in fig. 2(a&b).

CoMFA and CoMSIA Contour Map analysis

The steric and electrostatic fields of QSAR based on PLS (partial least square analysis) standard deviation coefficients were plotted as 3Dimensional contour maps with specific color codes of CoMFA and CoMSIA are depicted in fig. 3(a&b).

The default contribution levels were set to 80% for favored region and 20% for the disfavored region during contour analysis. The CoMFA contour map helps in finding the constructional requirements of the aligned analogues, steric (green and yellow) and electrostatic (red and blue) contributions that imply the respective, favorable or unfavorable and besides electron positivity and negativity favored with the interacting receptor. For CoMSIA along with steric and electrostatic fields, we can also use Hydrophobicity, and Hydrogen bond donor and acceptor descriptors as their structural requirements.

These 5 important (steric and electrostatic) characteristics of CoMFA and CoMSIA contour map describes the regions where a substituent has been able to increase or decrease the biological potency of a molecule which we use to suggest the possible modification of the existing molecules.

Table 2(a): Training set compounds with experimental and predicted activities and docking score

Molecule number	Actual PIC50	CoMFA		CoMSIA		Dock score
		Predicted PIC50	Residuals	Predicted PIC50	Residuals	
2	8.52	8.36	0.16	8.27	0.25	-22.7
3	9	9.01	-0.01	9.04	-0.04	-27.8
4	8.4	8.32	0.08	8.36	0.04	-18.7
5	8.52	8.46	0.06	8.45	0.07	-24.5
9	8.7	8.7	0	8.71	-0.01	-20.8
10	8.7	8.74	-0.04	8.75	-0.05	-20.4
11	8.52	8.59	-0.07	8.596	-0.076	-23.2
12	8.4	8.47	-0.07	8.45	-0.05	-21.7
14	9.1	9.05	0.05	8.88	0.22	-22.9
16	7.74	7.7	0.04	7.696	0.044	-15.9
17	9	8.95	0.05	9.01	-0.01	-20.3
19	9	8.92	0.08	9.07	-0.07	-22.5
21	9	8.96	0.04	8.97	0.03	-23.3
26	9	8.97	0.03	8.93	0.07	-20.8
27	9	8.999	0.001	8.95	0.05	-20.9
28	9	9.04	-0.04	9.22	-0.22	-20.3
30	9	8.97	0.03	9	0	-19.7
32	7.28	7.48	-0.2	7.39	-0.11	-18.8
33	9	9.02	-0.02	8.9	0.1	-21.9
34	9	9.11	-0.11	8.92	0.08	-21.6
35	9	9.02	-0.02	8.96	0.04	-22.7
37	8.7	8.6	0.1	8.66	0.04	-19.9
38	8.52	8.56	-0.04	8.61	-0.09	-19.6
40	8.52	8.71	-0.19	8.54	-0.02	-24.5
41	9	8.97	0.03	8.94	0.06	-28.1
42	9	8.91	0.09	8.88	0.12	-30.9
43	9	9.11	-0.11	8.98	0.02	-31.6
44	8.7	8.62	0.08	8.65	0.05	-22.2
45	9	9.05	-0.05	9	0	-29.7
46	9	8.99	0.01	9.1	-0.1	-26.5
47	9	9.01	-0.01	9.06	-0.06	-19.2
48	8.7	8.71	-0.01	8.83	-0.13	-20.6
49	9	8.96	0.04	9	0	-24.2
50	7.21	7.47	-0.26	7.49	-0.28	-23.1
51	7.92	7.78	0.14	7.86	0.06	-22.7
53	7.15	7.18	-0.03	7.29	-0.14	-23
54	7.92	7.78	0.14	7.72	0.2	-25
55	7.55	7.5	0.05	7.45	0.1	-26.6
56	7.46	7.15	0.31	7.28	0.18	-23
57	7.92	7.96	-0.04	7.999	-0.079	-23
58	7.66	7.56	0.1	7.5	0.16	-23.8
59	7	7.27	-0.27	7.37	-0.37	-22.3
60	7.82	7.88	-0.06	8.05	-0.23	-21.7
61	7.85	7.82	0.03	7.74	0.11	-22.9
62	7.96	7.82	0.14	7.74	0.22	-22.9
63	7.68	7.93	-0.25	7.93	-0.25	-22.4
66	8.05	8.02	0.03	8.03	0.02	-22
68	7.92	7.88	0.04	7.89	0.03	-22.5
69	8.1	8.14	-0.04	8.25	-0.15	-22.5
72	7.92	7.83	0.09	7.799	0.121	-21.7
75	8.22	8.29	-0.07	8.12	0.1	-27.9
76	7.51	7.59	-0.08	7.45	0.06	-23.5
78	8.3	8.25	0.05	8.15	0.15	-26.2
79	8.1	8.14	-0.04	8.18	-0.08	-23.7
80	7.51	7.47	0.04	7.62	-0.11	-22.5
81	7.68	7.8	-0.12	7.67	0.01	-27.4
84	7.12	7.1	0.02	7.09	0.03	-25.4
86	7.21	7.09	0.12	7.18	0.03	-25
87	7.47	7.68	-0.21	7.71	-0.24	-17.9
88	7.77	7.7	0.07	7.65	0.12	-18.4
89	7.96	7.89	0.07	8.03	-0.07	-19.3
90	7.77	7.78	-0.01	7.86	-0.09	-19.7
92	7.57	7.51	0.06	7.55	0.02	-22.9
95	7.85	7.845	0.005	7.88	-0.03	-20.7
97	6.15	6.18	-0.03	6.17	-0.02	-18.2
100	7.07	7.09	-0.02	6.95	0.12	-18.2

Table 2(b): Test set compounds with experimental and predicted activities and docking score

Molecule number	PIC50	CoMFA		CoMSIA		Dock score
		Predicted PIC50	Residual	Predicted PIC50	Residual	
1	9	8.44	0.56	8.53	0.47	-23.2
6	8.15	8.9	-0.75	8.39	-0.24	-20.0
7	8.22	8.42	-0.2	8.43	-0.21	-21.0
8	8.52	8.88	-0.36	8.44	0.08	-19.1
13	7.3	8.72	-1.42	8.46	-1.16	-19.4
15	8.22	9.05	-0.83	8.73	-0.51	-17.2
18	8.7	7.55	1.15	7.5	1.20	-19.3
20	8.7	7.66	1.04	7.8	0.90	-21.4
22	8.7	7.59	1.11	7.7	1.00	-20.2
23	8.22	8.88	-0.66	8.86	-0.64	-23.4
24	8.52	8.81	-0.29	8.65	-0.13	-18.7
25	8.3	8.99	-0.69	8.79	-0.49	-20.1
29	9	8.14	0.86	7.92	1.08	-19.4
31	8.4	8.88	-0.48	8.75	-0.35	-22.2
36	8.1	8.66	-0.56	8.68	-0.58	-22.8
39	8.3	8.68	-0.38	8.9	-0.60	-19.3
52	7.92	7.37	0.55	7.45	0.47	-23.5
64	8.4	7.71	0.69	7.79	0.61	-19.6
65	6.52	8.25	-1.73	8.23	-1.71	-20.6
67	6.6	8.09	-1.49	7.93	-1.33	-26.8
70	8.7	7.74	0.96	7.95	0.75	-20.2
71	8.7	8.02	0.68	8.13	0.57	-22.3
73	8.7	8.18	0.52	8.39	0.31	-21
74	8.7	7.66	1.04	7.47	1.23	-21.2
77	7.77	8.31	-0.54	7.94	-0.17	-30.6
82	7.89	7.34	0.55	7.61	0.28	-21.8
83	7	7.75	-0.75	8.15	-1.15	-22.5
85	6.89	7.77	-0.88	7.87	-0.98	-25.5
91	8.7	7.35	1.35	7.43	1.27	-19
93	6.72	7.84	-1.12	7.81	-1.09	-22.3
94	6.89	7.87	-0.98	7.83	-0.94	-21.8
96	8.7	6.85	1.85	7.12	1.58	-20.4
98	7.14	6.63	0.51	6.24	0.9	-18.3
99	8.22	7.22	1	6.88	1.34	-18.6

Table 2(c): Statistical results of CoMFA and CoMSIA

Components	CoMFA	CoMSIA
q ²	0.845	0.804
r ²	0.978	0.968
Number of components	5	6
Standard Error of Estimate	0.108	0.131
F-value	434.811	295.133
	Field Contributions (%)	Field Contributions (%)
Steric	54.5	17.4
Electrostatic	45.5	28.3
Hydrophobic	-	20.8
H-Donor	-	18.5
H-Acceptor	-	14.9

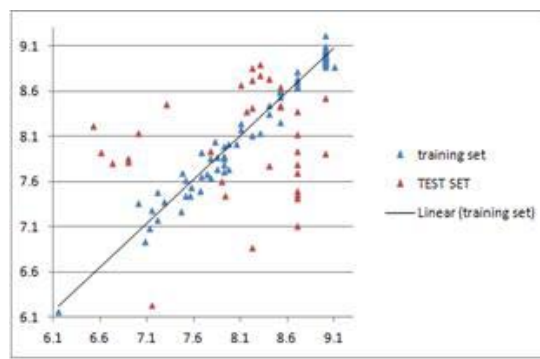
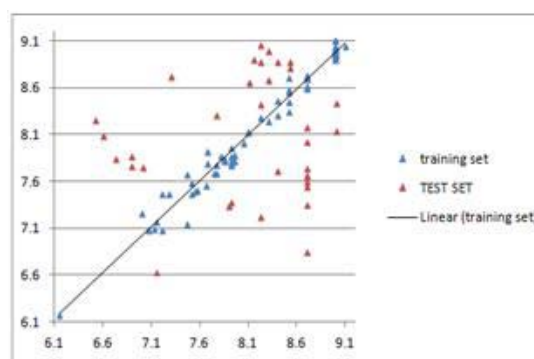


Fig. 2: Predictive vs. experimental pIC50 values derived from CoMSIA model for training set (blue) and test set (red)

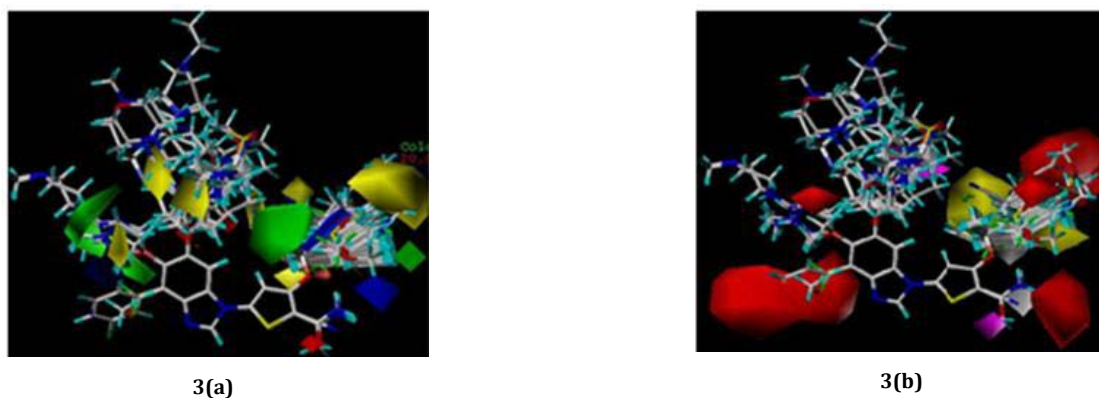


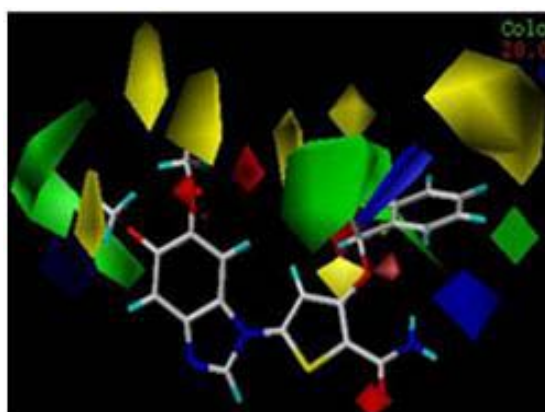
Fig. 3: Alignment of PLK1 inhibitors with contour maps (a) CoMFA (b) CoMSIA

CoMFA Contour Map analysis

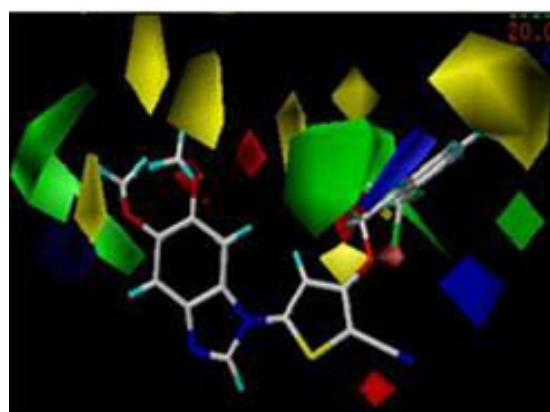
According to CoMFA steric field contour map, green colored polyhedral represents the area where a steric bulk substituent enhances the potency; while yellow colored polyhedral represents the area where a steric bulk substituent decreases the potency. Whereas the electrostatic field contour map, red colored polyhedral represents the area where electron negativity (substituent) enhances the potency; while blue colored polyhedral represents the

area electron positivity (substituent) will enhance the potency. The contour maps of steric and electrostatic fields of CoMFA are illustrated in following fig. 4(a) and (b).

The high (mol-14) and least enthusiastic (mol-97) compounds are served as reference molecules. Large green counter located at the 6th position of the thiophene substituted phenyl ring represents sterically favored that supports the fact that the molecules 1 to 12 are enhancing the biological activity.



4(a)



4(b)

Fig. 4: CoMFA steric & Electrostatic contours of PLK₁ inhibitor. In which green & yellow polyhedral indicates regions where more steric bulk group, while red & blue indicates regions.

Electrostatic contours of 1-12 compounds representing all compounds have about high (active) potency against PLK₁, because in R position all having alkyl or aryl alkyl groups; while in X position all have halogens or methyl halogens, which favor the electronegativity. In the amide position of a scaffold in Oxygen region electronegativity favored. Overall all these 12 compounds were increasing the biological potency as like *in vitro* studies that collected from the literature [20-22]. Steric contours of the same molecules representing that benzimidazole 6th position of methoxy groups are optimally favored for steric bulk groups. In thiophene attached with "O" is unfavorable and "O" substituted methyl is favored for the steric bulk groups. Thiophene substituted with phenyl ring where X position with halogens or methyl halogens have optimally favored, and the remaining positions of the respective ring are not favored for modifications, for example, the molecules 53, 59, 65, 67, 83, 84, 85 and 94.

According to the literature [20-22], 5th and 6th positions in Benzimidazole ring of the scaffold having effective steric contribution for the biological activity of the molecules that is clearly supported by the present 3D-QSAR studies. In 31 and 32 numbered

molecules where pyridine was substituted, at 5th and 6th positions benzimidazole showing effect on their activity. For 13-49 compounds, 13, 16 and 32 compounds not have that much biological potency for sterically bulk groups.

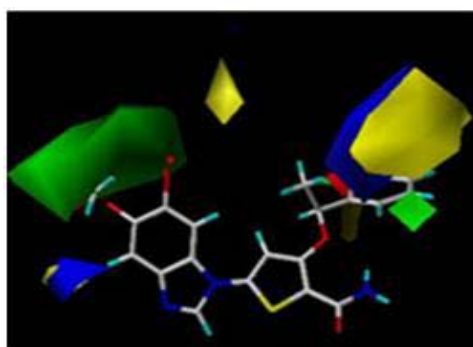
50-84 compounds electrostatic contours representing all the compounds have CN, oxymethyl, halogens or sulfate methyl groups in R₁ and R₂ positions. Compound 59, 65, 67, 83 and 84 have the CN or sulfate methyl groups which will affect the activity (least potency). Thiophene substituted with phenyl ring where R₁ 4th positions of the phenyl ring substituents affecting the activity, remaining all increasing the activity. Mostly, the 2nd position of the respective phenyl ring substituents of methyl, halogens and methyl halogenated groups are eventually enhancing the potency.

Electrostatic contours of 85-95 compounds representing that 89 and 91 have high potency and has the thionyl group attachment increasing the activity. The compounds 85, 93 and 94 have the least potency and remaining all are unadorned for steric bulk groups. In 96-100 compounds, 96 and 99 have lofty potency, and 97 and 98 have tiniest potency. The compounds which have high potency are favored for electronegativity.

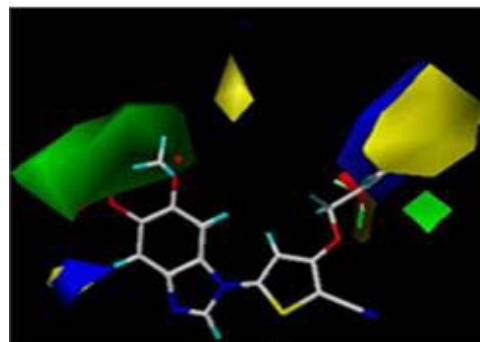
CoMSIA Contour Map analysis

The steric and electrostatic fields of CoMSIA contour maps have been connatural to the corresponding contour maps of CoMFA. The contour maps of steric & electrostatic, Hydrogen bond and hydrophobic fields have shown in following fig. 5(a), (b), (c), (d), (e) and (f). The high (mol-14) and least functioning (mol-97) compounds are served as

reference molecules. The green and lemon contours represent sterically adorned and unadorned regions, while cherry and blue for electro negativity and positivity favored, cyan and purple contour depict suitable and unsuitable for hydrogen bond donor groups, while magenta and red contours for favorable and unfavorable hydrogen bond acceptor groups and contours in yellow and white indicates hydrophobic and hydrophilic preferred regions.

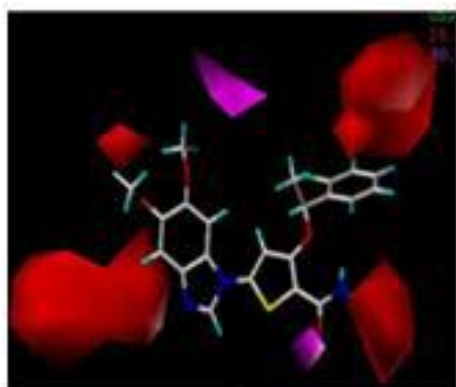


5(a)

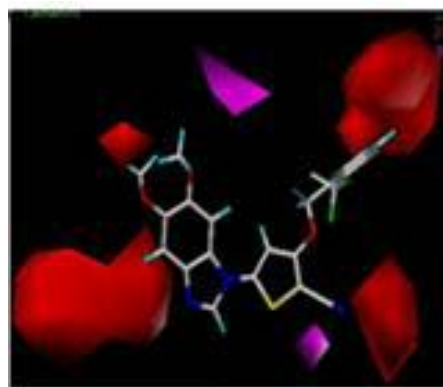


5(b)

Fig. 5a & b: CoMSIA steric & Electrostatic contours of PLK1 inhibitor. In which green & yellow polyhedral indicates regions where more steric bulk group, while red & blue indicates regions where more high (negative charge) & low electron density (positive charge) will enhance the bio-logical potency. (a) High potency compound-14 (b) Least potency compound-97

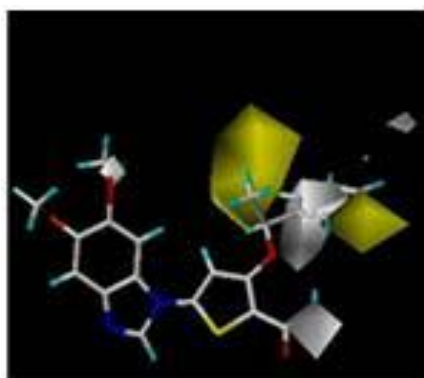


5(c)

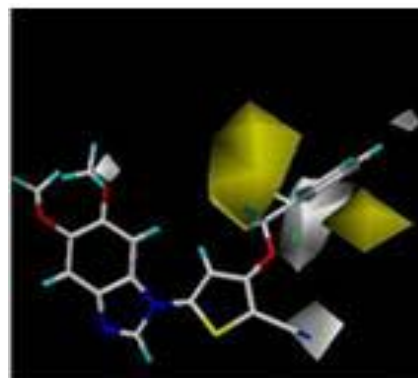


5(d)

Fig. 5c&d: CoMSIA Hydrogen bond donor & acceptor contours of PLK1 inhibitor. In which cyan & purple polyhedral indicates favorable & unfavorable for H-bond donor, while magenta & red polyhedral for favorable and unfavorable H-bond acceptor groups. (c) High potency compound-14 (d) least potency compound-97



5(e)



5(f)

Fig. 5e&f: CoMSIA Hydrophobic site (of hydrogen bond) contours of PLK1 inhibitor. In which yellow and white polyhedral indicates hydrophobic and hydrophilic favorable regions. (e) High potency compound-14 (f) least potency compound-97

Molecular docking

Molecular Docking also well supported the 3D-QSAR analysis with better docking scores having good interactions with the predefined active site. Docking score and interactions based on RMSD having low energy conformation was listed in the Table: 2(a&b). The highest active molecule shows good results when compared with the least active molecule. Highest active molecule shows interaction with Phe183 and Cys133 with distance 1.66, 2.66, 2.21 and 1.55, 1.52 respectively. While reference molecule 3THB shows interactions with Cys133 and Asp194. Were represented in fig. 6.

Prediction of novel molecules

The highly active compound (mol: 14) used for suggesting the favorable systematic requirements of the next-generation lead molecules, based on above 3D-QSAR analysis. "O" attached to thiophene ring substituted methyl & 6th position of thiophene substituted phenyl ring is selected for new structural requirements. The novel lead molecules and the predicted biological activities

listed in the table 3, which was validated by molecular docking and found to be more potent than previous molecules.

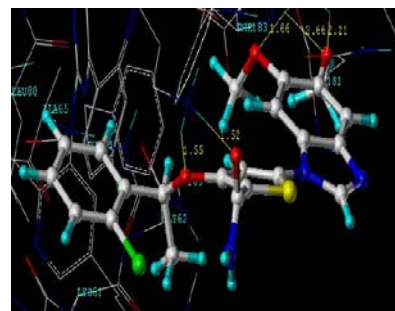


Fig. 6: Docking of highly active compound with Active Site of 3THB

Table 3: Assumed new categories of thiophene derivatives as PLK1 inhibitors

Molecule no	Predicted pIC ₅₀	Structure of molecule
1	9.4348	
2	9.35093	
3	9.32946	
4	9.29203	
5	9.478	

CONCLUSION

In conclusion, our present studies have established that CoMFA and CoMSIA models have provided satisfactory statistical results in terms of q² and r² values for represented thiophene derivatives. Both CoMFA and CoMSIA models showed significant correlations of biological activities with steric, electrostatic, hydrophobic, hydrogen bond donor and acceptor fields, establishing the significance of all these parameters in the selectivity and activity of the compounds. However, in comparison to CoMSIA the CoMFA analysis showed slightly better statistical models and the reliability of both the models was verified by using the test set compounds. These results shed light on some important sites, where steric, electrostatic, hydrophobic, hydrogen-bond donor and hydrogen-bond acceptor modifications

should significantly affect the bioactivities of the compounds. The 3D contour plots derived from the CoMFA, CoMSIA and docking provided vital clues which helped us to design 5 novel molecules with improved PLK1 inhibitory activity. These molecules showed new insights on effective therapeutic agents against these classes of enzymes.

CONFLICT OF INTERESTS

Declared None

REFERENCES

- Shannon RS, Nihal A. Polo-like kinase (PLK) 1 as a target for prostate cancer management. *FASEB J* 2005;57:677-82.

2. Ruddle RW. *Cancer Biology*. 3rd ed. Oxford University Press: New York; 1995. p. 10.
3. Hardman JG, Limbird LE, Gilman AG. In *Goodman's the pharmacological basis of therapeutics*. Eds. 10th ed. McGraw-Hill: New York; 2001. p. 1417.
4. Barr FA, Sillje HHW, Nigg EA. Polo-like kinases and the orchestration of cell division. *Nat Rev Mol Cell Biol* 2004;5:429-40.
5. Ma S, Charron J, Erikson RL. Role of PLK2 (Snk) in mouse development and cell proliferation. *Mol Cell Biol* 2003;19:6936-43.
6. Frank E, Juping Y, Klaus S. Polo-like kinases and oncogenesis. *Oncogene* 2005;24:267-76.
7. Liu X, Erikson RL. Polo-like kinase (PLK)1 depletion induces apoptosis in cancer cells. *Proc Natl Acad Sci USA* 2003;100:5789-94.
8. Elez R, Piiper A, Kronenberger B, Kock M, Brendel M, Hermann E, *et al.* Tumor regression by combination antisense therapy against PLK1 and Bcl-2. *Oncogene* 2003;22:69-80.
9. Takai N, Hamanaka R, Yoshimatsu J, Miyakawa I. Polo-like kinases (PLKs) and cancer. *Oncogene* 2005;24:287-91.
10. Wolf G, Elez R, Doermer A, Holtrich U, Ackermann H, Stutte HJ, Almannsberger HM, *et al.* Prognostic significance of polo-like kinase (PLK) expression in non-small cell lung cancer. *Oncogene* 1997;14:543-9.
11. Wolf G, Hildenbrand R, Schwar C, Grobholz R, Kaufmann M, Stutte HJ, *et al.* Polo-like kinase-a novel marker of proliferation: correlation with estrogen-receptor expression in human breast cancer. *Pathol Res Pract* 2000;196:753-9.
12. Knecht R, Oberhauser C, Strebhardt K. PLK (polo-like kinase), a new prognostic marker for oropharyngeal carcinomas. *Int J Cancer* 2000;89:535-6.
13. Tokumitsu Y, Mori M, Tanaka S, Akazawa K, Nakano S, Niho Y. Prognostic significance of polo-like kinase expression in esophageal carcinoma. *Int J Oncol* 1999;15:687-92.
14. Ito Y, Miyoshi E, Sasaki N, Kakudo K, Yoshida H, Tomoda C, *et al.* Polo-like kinase 1 over expression is an early event in the progression of papillary carcinoma. *Br J Cancer* 2004;90:414-8.
15. Gray PJ Jr, Bearss DJ, Han H, Nagle R, Tsao MS, Dean N, *et al.* Identification of human polo-like kinase 1 as a potential therapeutic target in pancreatic cancer. *Mol Cancer Ther* 2004;3:641-6.
16. Takai N, Miyazaki T, Fujisawa K, Nasu K, Hamanaka R, Miyakawa I. Expression of polo-like kinase in ovarian cancer is associated with histological grade and clinical stage. *Cancer Lett* 2001;164:41-9.
17. Takahashi T, Sano B, Nagata T, Kato H, Sugiyama Y, Kunieda K, *et al.* Polo-like kinase 1 (PLK1) is over expressed in primary colorectal cancers. *Cancer Sci* 2003;94:148-52.
18. Weichert W, Schmidt M, Gekeler V, Denkert C, Stephan C, Jung K, *et al.* Polo-like kinase 1 is over expressed in prostate cancer and linked to higher tumor grades. *Prostate* 2004;60:240-5.
19. Strebhardt K, Kneisel L, Linhart C, Bernd A, Kaufmann R. Prognostic value of polo-like kinase expression in melanomas. *JAMA* 2000;283:479-80.
20. Emmitte KA, Andrews CW, Badiang JG, Davis-Ward RG, Dickson HD, Drewry DH, *et al.* Discovery of thiophene inhibitors of polo-like kinase. *Bioorg Med Chem Lett* 2009;19:1018-21.
21. Emmitte KA, Adjabeng GM, Andrews CW, Alberti JG, Bambal R, Chamberlain SD, *et al.* Design of potent thiophene inhibitors of polo-like kinase 1 with improved solubility and reduced protein binding. *Bioorg Med Chem Lett* 2009;19:1694-7.
22. Rheault TR, Donaldson KH, Badiang-Alberti JG, Davis-Ward RG, Andrews CW, Bambal R, *et al.* Heteroaryl-linked 5-(1H-benzimidazol-1-yl)-2-thiophenecarboxamides: potent inhibitors of polo-like kinase 1 (PLK1) with improved drug-like properties. *Bioorg Med Chem Lett* 2010;20:4587-92.